

# Biomechanical Modeling of Human Foot using Finite Element Methods

E. Vijayaragavan\* and T. V. Gopal

Department of Mechanical Engineering, SRM University, Kattankulathur – 603203, Tamil Nadu, India;  
vijayaragavan.e@ktr.srmuniv.ac.in, gopal.t@ktr.srmuniv.ac.in

## Abstract

**Objective:** Studies involving in vivo experimentation in human beings requires ethical clearance, and it is cumbersome due to existing laws and procedures. This research aims at developing a 3D anatomically realistic model of the ankle joint and the foot. **Methodology:** The Computed Tomography (CT) images of the human foot were captured. Using image reconstruction technique, the outer surface of the various components of the foot including the 26 bones, plantar fascia, Achilles tendon and other ligaments were developed. **Findings:** Applying the necessary boundary and loading conditions on the mechanical model, the internal stress distribution under different conditions of the foot were calculated and compared with published literature. **Applications/Improvements:** Upon validation, this model can be used to study the behavior a deformed/diabetic foot by altering suitable material properties of the foot. Further, the detailed study on the design of custom foot orthoses may be performed to counter effect the foot deformity.

**Keywords:** Finite Element (FE) Model, Human Foot, Image Reconstruction

## 1. Introduction

The in-vivo study on testing of implants, prostheses and other fixation devices in human requires the ethical approval. In some cases, the experiments are done in animals to provide the physiopathological response in living bodies<sup>1</sup>. These results cannot be directly used to solve human behavior since the properties of the tissues and its functions are different. To overcome the above challenge, a musculoskeletal model of the human body has to be developed which would act as a powerful tool to study its biological structures<sup>2</sup>. Many researchers<sup>2-6</sup> are working in developing the finite element model of the human joints which enables to study the biomechanical interactions of each part and the internal displacement of the components with reference to the external stimulus. This study attempts to develop a finite element model of the human ankle-foot complex. The input for the finite element model were obtained from the medical imaging techniques like Magnetic Resonance Imaging (MRI) and Computed Tomography (CT). These methods are used to

capture the anatomical structure of the humans. Though both MRI and CT offer the advantage of capturing the soft tissues like tendons and ligaments in the foot as well as the hard bony structures, generally CT is preferred over MRI as it is economical<sup>7-10</sup>.

The foot is a multi-bone structure with many joints and movements. It combines mechanical complexity and structural strength. Anatomically the human foot contains 26 bones, 33 joints, 107 ligaments and 19 muscles<sup>11,12</sup>. All these components must work in unison to provide support, balance, and mobility. A structural deformity or any malfunction of the foot results in the development of problems elsewhere in the body; similarly, an abnormality in any other parts of the body leads to problems in the feet<sup>13,14</sup>. The common foot abnormalities in humans are the flat foot, weakened transverse arch, hallux valgus, hammer toe, talipes, pescavus, hump foot, hollow claw foot<sup>12</sup>. The structural arrangement of the healthy human foot is depicted in Figure 1.

Study on the effects of structural characteristics of the bones in the foot on plantar pressure distribution and

\*Author for correspondence

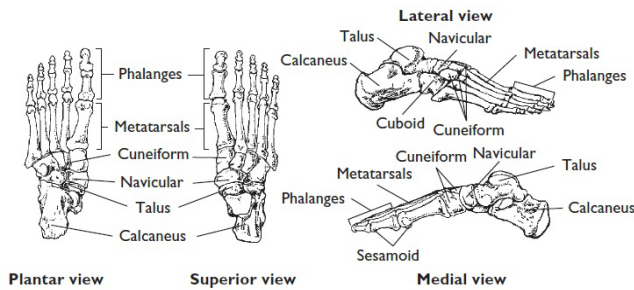


**Figure 1.** Anatomy of foot.

stress concentration in the bones are very much required for individualized treatment for various foot deformities<sup>15</sup>. As the body propels forward during locomotion, one of the legs acts as a support enabling another leg to proceed forward for a new location<sup>16</sup>. Then the roles of legs will be reversed that assists in locomotion. The gait cycle starts when one foot makes contact with the ground and ends when that same foot contacts the ground again. Few<sup>17-22</sup> has performed human foot analysis based on experimental work using pressure sensors, pedobarograph and gait analysis setup. These experiments do not well support the lack of technological advancement in the experimental measurements, the mechanism for load transfer and stress in the inner cross section of the bones. In tune with this problem, many researchers<sup>23-26</sup> are working in developing a virtual model of biological systems, with which the finite element analysis can be performed on these models to study its behavior in the given loading conditions. In addition to the stress distribution in the foot complex, the stress-strain relation and the deformation or growth pattern of the foot can be studied. This study aims at developing a comprehensive finite element model of the foot by reconstructing the CT images. In addition to the 26 bones of the foot, the Achilles tendon, plantar fascia, and few ligaments were also modeled. This model would help us in finding the effect of the change in stiffness of the soft tissues on internal stress distribution and mechanism of load transfer in the foot.

## 2. Image Reconstruction

As per the approval from the Institutional Ethics Committee vide clearance number 965/IEC/2016, a female subject (21 years, 136 cm and 600 N) with no history of foot deformities is selected for this study. After The subject is explained about the process and after obtaining

the consent form, Computed Tomograms (CT) of the left foot were acquired using a SIEMENS Somatom Spirit with a slice thickness of 1 mm as shown in Figure 2.



**Figure 2.** SIEMENS Somatom Spirit Scanner.

The digitized CT images were imported into image processing software MIMICS v10 (Materialise, Leuven, Belgium) for reconstruction and to obtain the skeleton boundary and the surface of the soft tissues as shown in Figure 3.

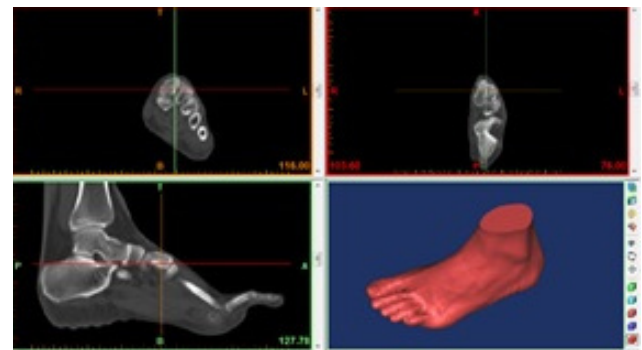


**Figure 3.** CT images imported in Mimics.

Based on threshold values, the surface model of the individual bones in the foot are generated using windowing and segmentation. The bones in the hindfoot, midfoot and forefoot are differentiated by providing different colors for better visualization as shown in Figure 4.

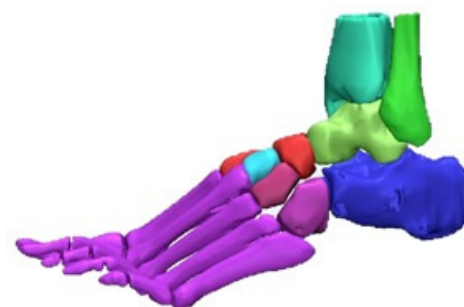


**Figure 4.** Individual bones of the foot.

The contours of the various entities in the foot like the bones, Achilles tendon, plantar fascia, inferior tibiofibular ligaments, posterior ligaments and soft are gathered by adjusting the threshold values. These entities are edited to smooth out its complex profile. Smoothing operations were performed to remove the stacks due to 1 mm cut in CT images. Each layer is edited with reference to its adjacent layer and the solid model thus obtained is shown in Figure 5. This process preserves the anatomical features of the various components of the foot. By treating the outer



**Figure 5.** Complete model of foot.

surfaces of the skeleton and soft tissues, the solid of the foot including all the bones were modeled.

### 3. Finite Element Modeling

The model thus developed by image reconstruction was imported and processed in the FE package ANSYS 15. The solid model of the foot, as shown in Figure 5 contains 28 bones including the distal segments of tibia and fibula and the 26 bones of the foot. The phalanges were connected by the cartilage and other connective tissues.

The contact surfaces were defined between the various bones in the foot, and it allows the relative articulating movement. The contact between the joint surfaces are assumed to be frictionless and are represented using the surface-to-surface contact in ANSYS. The Achilles tendon, talo navicular ligament, deltoid ligament and the plantar fascia were meshed with 3D tetrahedral elements as shown in Figure 6.

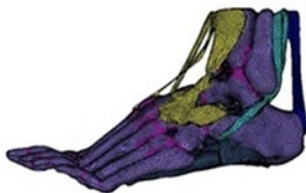


**Figure 6.** Meshed model of the foot.

## 4. Material Properties

Even though the properties of foot vary along different location, for simplicity, the homogeneous property is assumed for all its components. Linear and elastic solid elements were selected for the components. The material properties of various elements of the foot were adopted from the published literature<sup>27-30</sup> and are listed in Table 1.

**Table 1.** Material Properties

Component	Modulus of elasticity (MPa)	Poisson's ratio	Element type
Bone	7300	0.3	3D tertahedron
Soft tissue	0.15	0.4	3D tertahedron
Cartilage	1	0.4	3D tertahedron
Ligament	260	0.4	3D tertahedron
Plantar Fascia	350	0.4	3D tertahedron
Ground support	20000	0.1	3D brick

## 5. Loading Conditions

For the different ambulatory activities of the foot the loading conditions are very complex, hence, in this study the standard bare foot gait during stance phase is considered. The motions in the varus-valgus and inversion-eversion angles were not considered as it is very small compared to the dorsi-plantar flexion angle. For performing the finite element analysis, the top surface of the ankle joint comprising of distal tibia and fibula along with the soft tissues were fixed. During Balanced Standing (BS) phase of the Gait cycle, the ankle joint is assumed to be in neutral position. A vertical force of 300 N representing half of the body weight is applied on each foot<sup>31-33</sup>. In addition to this load, 150 N is applied to Achilles tendon during balanced standing<sup>34</sup>. This force is represented by five equivalent vectors at the posterior extreme of the calcaneus. The loading condition of the foot is depicted in Figure 7.

## 6. Results and Discussion

For performing element analysis of the human foot, a 3D anatomical model is developed by image reconstruction. Under the stated loading and boundary conditions, the model thus developed can be

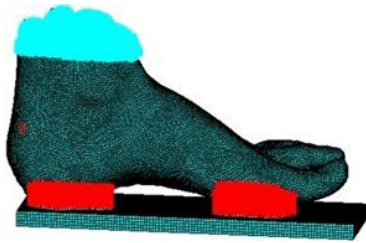


**Figure 7.** Loading conditions in human foot.

used for studying the stress distribution in the foot. Figure 8 depicts the Von Mises stresses in the foot during balanced standing.

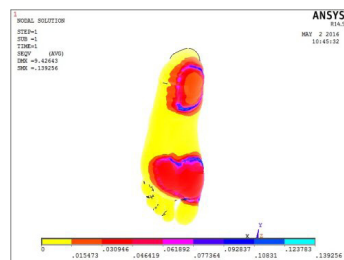


**Figure 8.** Von Mises stresses in the foot.

A peak stress of 0.139 MPa is observed in the heel region and the metatarsals experiences stresses ranging from 0.015 to 0.07 MPa. Similar FE analysis is performed for heel strike and toe-off phases, and the results are listed in Table 2 and depicted in Figure 9.

**Table 2.** Internal stress from FEA

Conditions	Stress (kPa)
Balanced standing (BS)	139
Heel strike (HS)	53
Toe off (TO)	210

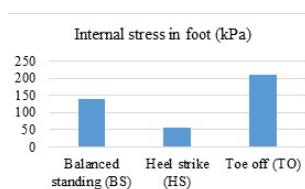


**Figure 9.** Internal stress in foot.

## 7. Conclusion

A 3D finite element model of the human foot which replicates/resembles the actual foot was developed in this study by stacking the CT slices by image reconstruction technique. The various components including the

26 bones, deltoid ligament, plantar fascia and achilles tendons were modeled which would be a new milestone achieved in this topic of interest. The subject-specific model is generated based on their geometry, and the corresponding loading conditions were applied to study the internal stress distribution in the foot for Balanced Standing (BS), Heel Strike (HS) and Toe-off (TO) phases during locomotion. The results conclude that the stress gradually increases from the HS (53 kPa), BS(139 kPa) and TO (210 kPa) respectively.

This model can be further validated by comparing the internal stress distribution calculated by experimental testing with the use of insoles or force plates for different phases of human locomotion.

## 8. Acknowledgement

This work is carried out in accordance with Institutional Ethics Committee vide clearance number 965/IEC/2016. The Authors thank Dr. Shantanu Patil – Head of the Department of Translational Medicine and Research, SRM University for his guidance in ethical clearance and offering valuable suggestions and feedback for this study.

## 9. References

1. Giridharan NV, Kumar V, Muthuswamy V. Use of Animals in Scientific Research. New Delhi: Indian Council of Medical Research, 2000 May.
2. Rosenberg ZS, Cheung Y, Jahss MH. Computed tomography scan and magnetic resonance imaging of ankle tendons: an overview. Foot Ankle. 1988 Jun; 8(6):297–307.
3. Bandak FA, Tannous RE, Toridis T. On the development of an osseo-ligamentous finite element model of the human ankle joint. International Journal of Solids and Structures. 2001; 38:1681–97.
4. Cheung JT, Zhang M. Finite Element Modeling of the Human Foot and Footwear. ABAQUS Users' Conference, 2006 May 23; Cambridge, USA. 2006. p. 145–59.
5. Qiu TX, Teo EC, Yan YB, Lei W. Finite element modeling of a 3D coupled foot–boot model. Medical Engineering and Physics. 2011 Dec; 33(10):1228–33.
6. Latif AA, Moazemi AG, Ali P, Misagh I, Abouei MA. Finite element analysis of human femur by reverse engineering modeling method. Indian Journal of Science and Technology. 2015 Jul; 8(13):1–10. Doi: 10.17485/ijst/2015/v8i13/47884.
7. Vickie B, Rocco P, Robert M, Peter H, Iain A. The use of sparse CT datasets for auto-generating accurate FE models

- of the femur and pelvis. *Journal of Biomechanics*. 2007; 40(1):26–35.
8. Martin G, Margit G, Christian P. Alternative solution of virtual biomodeling based on CT-scans. *Journal of Biomechanics*. 2009 Aug; 42(12):2006–2009.
  9. Bernard G, Germain F, Hugues B, Frederic C, Patrick C, Denis F, Alban G, Patrick H, Carole L, Herve L, Johan M, Joachim T, Tristan G. OntoVIP: An ontology for the annotation of object models used for medical image simulation. *Journal of Biomedical Informatics*. 2014 Dec; 52:279–92.
  10. Madhulika B. A Proposed Stratification Approach for MRI Images. *Indian Journal of Science and Technology*. 2015 Sep; 8(22):1–10. Doi: 10.17485/ijst/2015/v8i22/72152.
  11. Cheryl LR. Anatomy of the ankle and foot. *Physical Therapy*. 1988 Dec; 68(12):1802–14.
  12. Hall SJ. *Basic Biomechanics*. 6th ed., Columbus: McGraw-Hill; 2012; 251–7.
  13. Diane LF. *Human and Nonhuman Bone Identification: A Color Atlas*. Florida: CRC Press; 2009; 477–504.
  14. Scholl WM. *The Human Foot - Anatomy, Deformities and Treatment*. Chicago: Foot Specialist Publishing Co.; 1916.
  15. Jason TC, Ming Z, Aaron KL, Fan YB. Three-dimensional finite element analysis of the foot during standing—a material sensitivity study. *Journal of Biomechanics*. 2005 May; 38(5):1045–54.
  16. Ashutosh K, Vipin S, Jain YK, Surender D. Review of Gait cycle and its parameters. *International Journal of Computational Engineering and Management*. 2011 Jul; 13:78–83.
  17. Cavanagh PR, Rodgers MM, Iiboshi A. Pressure Distribution under Symptom-Free Feet during Barefoot Standing. *Foot and Ankle International*. 1987 Apr; 7(5):262–8.
  18. Lavery LA, Vela SA, Fleischli JG, Armstrong DG, Lavery DC. Reducing plantar pressure in the neuropathic foot – a comparison of footwear. *Diabetes Care*. 1997 Nov; 20(11):1706–10.
  19. Rasovic A, Newcombe L, Lloyd J, Dalton E. Effect of customized insoles on vertical plantar pressures in sites of previous neuropathic ulceration in the diabetic foot. *The Foot*. 2000 Sep; 10(3):133–8.
  20. Manikandan K, Logesh K, Sivaraman J, Padmapriya P, Vijayalakshmi C. Design and development of a foot pressure scanner for diabetic patients. *Indian Journal of Science and Technology*. 2016 Jan; 9(2):1–4. Doi: 10.17485/ijst/2016/v9i2/85808.
  21. Manjunatha VG, Kamalesh VN. Vision based Human Gait Recognition System: Observations, Pragmatic Conditions and Datasets. *Indian Journal of Science and Technology*. 2015 Jul; 8(15):1–11. Doi: 10.17485/ijst/2015/v8i15/71237.
  22. Lee H, Jang E, Kim J, Hong J, Yu J, Lee D. A Study of Postural Sway according to the Wedge Direction during one Leg Standing. *Indian Journal of Science and Technology*. 2016 Jul; 9(25):1–9. Doi: 10.17485/ijst/2016/v9i25/97237.
  23. Vijayaragavan E, Leya MK, Sulayman H, Gopal TV. Application of rapid prototyping in the treatment of clubfoot in children. *Procedia Engineering*. 2014 Dec; 97:2298–305.
  24. Kai T, Dongmei W, Chengtao W, Xu W, Anmin L, Christopher J, David H. An in vivo experimental validation of a computational model of human foot. *Journal of Bionic Engineering*. 2009; 6:387–97.
  25. Vara I, Evan D, Joseph MI, Bruce JS, William RL. Finite element analysis of the foot: Model validation and comparison between two common treatments of the clawed hallux deformity. *Clinical Biomechanics*. 2012; 27:837–44.
  26. Ranjitha RJ, Vijayaragavan E, Angeline K. 3dimensional modeling of an ankle foot orthosis for Clubfoot deformity. *International Journal of Biomedical Research*. 2011; 2:171–80.
  27. Chen WP, Tang FK, Ju CW. Stress distribution of the foot during mid-stance to push-off in barefoot gait - a 3D finite element analysis. *Clinical Biomechanics*. 2001 Aug; 16(7):614–20.
  28. Tao K, Wang D, Wang C, Wang X, Liu A, Nester CJ, Howard D. An In Vivo Experimental Validation of a Computational Model of Human Foot. *Journal of Bionic Engineering*. 2009 Dec; 6(4):387–39.
  29. Wright DG, Rennels DC. A study of the elastic properties of plantar fascia. *The Journal of Bone and Joint Surgery*. 1964 Apr; 46(3):482–92.
  30. Thomas AS, Ahmet E, Susan ES, Ann Y, Scott T, Peter RC. Simple finite element models for use in the design of therapeutic footwear. *Journal of Biomechanics*. 2014; 47:2948–55.
  31. Shane J, Haihua O. Effects of boundary conditions on foot behavior in the standing position in 3D finite element foot model. *Journal of Foot and Ankle Research*. 2014 Apr; 7(1, A38).
  32. Shanti J, Patil KM, Brank LH, Huson A. Stresses in a 3D two arch model of a normal human foot. *Mechanics Research Communications*. 1996 Jul; 23(4):387–93.
  33. Jason TC, Ming Z, An KN. Effect of Achilles tendon loading on plantar fascia tension in the standing foot. *Clinical Biomechanics*. 2006 Feb; 21(2):194–203.
  34. Simkin. Structural analysis of the human foot in standing posture. Ph.D. dissertation, Department of Biomechanics, Tel Aviv University, Aviv-Yafo, Israel, 1982.